

April 2006

Observation of Betatron Motion In the Rutgers 12-Inch Cyclotron

Timothy W. Koeth[†], Stuart C. Hanebuth, William Schneider
Rutgers University, Piscataway NJ 08854

Daniel Hoffman
Princeton University, Princeton NJ

ABSTRACT: A small 12-Inch, 1.2MeV proton cyclotron was constructed for instructional use in an upper level Physics lab course.[1] The authors and seven undergraduate students participated in the improvement of the 12-inch cyclotron. Weak focusing pole tips, an improved ion source, a retrofitted faraday cup, and increased RF power facilities have enabled the first visible (on a

fluorescent screen) beam with the 12-inch magnet. Furthermore, clear vertical beam spot oscillations as a function of radius demonstrate betatron motion and confirm the expected performance of the shaped pole tips. These vertical oscillations signal the need to provide either better DEE alignment or the installation of “pullers” in the DEE aperture.

I. INTRODUCTION. Early work on the 12-inch cyclotron was performed with a 9-inch magnet to facilitate progress while the 12-inch magnet was being prepared for service. The faces of the 9-inch pole tips were parallel within 0.0001 inches – no effort of shaping the field for focusing was expended. Ions were produced with a crude filament near the top lid of the cyclotron chamber, and the entire chamber was filled with hydrogen gas. Even with a maximum RF power of just 50 watts, thus a DEE V_{p-p} of 3300V, beam currents on the order of 10nAmps of 0.60 MeV protons were reproducibly achieved with the 9-inch magnet. It was initially believed that the characteristic behavior of the cyclotron’s operation would continue in the 12-inch magnet.

The upgrade from the 9-inch magnet (known as the 9-inch prototype) to the present 12-inch magnet was to realize the goal of producing 1.2MeV protons. The experimenters were quickly disappointed when only fractions of a nAmp beam were achieved in the larger magnet. Much effort was put into understanding the problem. First, pole tips with a slight radial taper to promote focusing were designed, installed and characterized [2,3]. Still with only a slight increase in beam current with the installation of the new pole tips, the ion source came under suspicion. An analysis of the simple ion source suggested that the DEE’s high voltage was suppressing electron emission and thus suppressing ion generation during the appropriate RF phase. A new ion source employing a chimney and gas delivery system

was designed. [4] Once sufficient RF power was available, such that the first ion revolution would clear the ion source chimney record beam intensity was immediately observed. In addition to the increased beam intensity, vertical beam position at different radii demonstrated betatron motion arising from the “weak focusing” pole tips. In order to document completely the understanding of the observed phenomena, we review the theory of beam dynamics; mainly for vertical betatron motion. We determine the 12-inch magnets’ field index, $n(r)$, and discuss improvements to the ion source and faraday cup. Finally we show observed betatron motion and compare it to theoretical expectations.

II. FOCUSING THEORY REVIEW. A quick review of orbit theory in a magnetic field which decreases with growing radius. This is colloquially known as weak focusing.

First we define the field index:

$$n = -\frac{r}{B} \frac{dB}{dr}$$

There are three possible cases:

1. $n < 0$ the field increases with r
2. $n = 0$ the field is uniform
3. $n > 0$ the field decreases with r

Vertical Stability: Expand B_r by a Taylor expansion:

$$B_r = z \left. \frac{\partial B_r}{\partial z} \right|_{z=0} + \frac{z^2}{2} \left. \frac{\partial^2 B_r}{\partial z^2} \right|_{z=0} + \dots$$

[†] Primary author: e-mail koeth@physics.rutgers.edu

We consider only the first term of this expansion. From Maxwell's equations, we know:

$$\vec{\nabla} \times \vec{B} = 0$$

In considering azimuthal symmetry, we can say:

$$\left. \frac{\partial B_r}{\partial z} \right|_{z=0} = \left. \frac{\partial B_z}{\partial r} \right|_{z=0}$$

thus

$$B_r = z \left. \frac{\partial B_r}{\partial z} \right|_{z=0} = z \frac{\partial B_z}{\partial r} = \frac{\partial B}{\partial r} z$$

Because $\left. \frac{\partial B}{\partial r} z \right|_{z=0}$ has no radial component we can say $B_z = B$. From the above definition of the field index we write:

$$B_r = \frac{\partial B}{\partial r} = -nB \frac{z}{r}$$

Any field change in one axis corresponds to a change in the other. Thus if we can measure the change in the vertical component of the B-field we can make an inference of the change in the horizontal component.

Now, let us write the equations of motion for a particle of mass m in the magnetic field. First consider the restoring force that the particle will experience when taking an excursion from the median plane. We assume the force is proportional to the displacement:

$$F = m\ddot{z} = Kz$$

Then next consider the guiding field:

$$F_z = -qv_\theta B_r$$

where

$$v_\theta = \omega r$$

Substitute for B_r and equate to get

$$m \frac{d^2 z}{dt^2} = -qvnB \frac{z}{r}$$

Re-arrange and again use $v_\theta = \omega r$ along with

the cyclotron equation $m = \frac{qB}{\omega}$, and we get the

well known Kerst-Serber Equation:

$$\frac{d^2 z}{dt^2} + n\omega^2 z = 0$$

A solution of $z = 0$ is the unperturbed orbit, but another, and more interesting, solution is:

$$z = z_{\max} \sin(\sqrt{n}\omega t)$$

Thus, for positive n , the particles oscillate about the midplane with an amplitude of z_{\max} and frequency of:

$$\omega_z = \sqrt{n}\omega$$

where ω is the orbit revolution frequency (the RF frequency). We then define ν_z :

$$\nu_z = \frac{\omega_z}{\omega} = \sqrt{n}$$

ν_z , the number of "betatron" oscillations per revolution, is called the "tune."

$\frac{d^2 z}{dt^2} + n\omega^2 z = 0$ does not place an upper limit on n and the more positive n is, the greater the "restoring force" $\omega^2 n z$ will become.

Radial Stability: For a thorough treatment of the properties of radial stability, the reader is referred to a previous document on the characterization of the 12-inch magnetic field [3]. Since this document primarily focuses on vertical motion, it suffices to restate the final equations of radial stability. The frequency of radial oscillation about the idea orbit is:

$$\omega_x = \omega\sqrt{1-n}$$

So the radial betatron "tune" is:

$$\nu_x = \frac{\omega_x}{\omega} = \sqrt{1-n}$$

Interestingly, in the radial focusing case, there is no lower limit on the value of n , it is only required that n remain below a value of 1 for radial stability, the smaller the n value, the greater the radial restoring force.

Complete transverse stability. It has thus been shown that for axial stability, n must be greater than 0, and for radial stability n must be less than 1. Total transverse stability exists in the region of:

$$0 < n < 1$$

For details beyond the scope of this document, coupled resonances between the transverse motions further limit the value of n . n values of 0.2, 0.25, 0.33, 0.5 (and others higher) need to be avoided. Since, the ions to be accelerated begin at $r = 0$, $n = 0$ and will only climb as the radius increases. If $n = 0.2$ needs to be avoided, then the rate at which B_z decreases must be moderated such that only near the maximum ion radius does n approach 0.2. (for further details, the interested reader is referred to Livingood[5])

The following measurements and modeling indeed confirm, at least in the assumption of azimuthal symmetry that our 12-inch magnet's field index runs from 0 to about 0.2 throughout the useful region for ion acceleration.

III. DETERMINATION OF FIELD INDEX.

After the installation of the tapered pole tips, McClain and Friedman characterized the vertical component of magnetic field as a function of radius at different levels of excitation.[2]

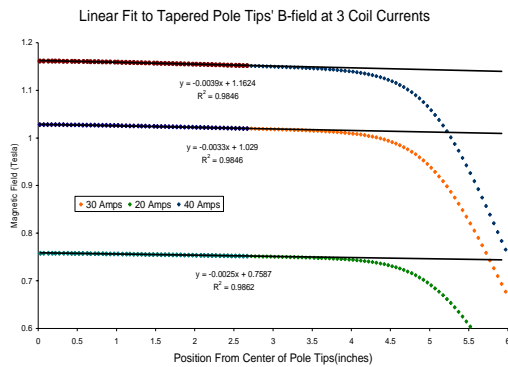


Fig.1 Radial measurements at three different magnet currents: 20, 30, & 40A

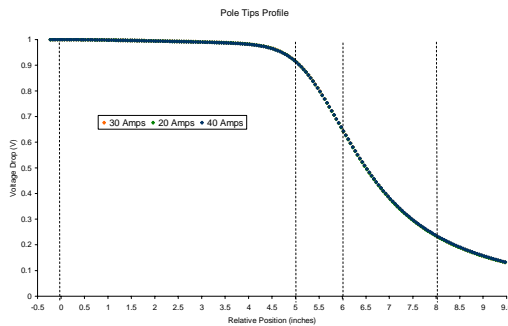


Fig.2 Simultaneous normalized field plot of the three current values: 20, 30, and 40 Amperes. The vertical dashed lines indicate, $r = 0$ – the center, $r = 5$ – the maximum ion radius, $r = 6$ – the pole tip edge, and $r = 8$ – the reference point.

The profiling of the radial dependence of the magnetic field between the pole pieces was executed with a Hall probe mounted on a computer controlled motorized platform. A LabView program wrote the Hall probes value and probe's position into a text file. For further details of the measurement the reader is referred to the work of McClain and Freidman. Figure 1 shows typical field profiles at different levels of magnetic excitation. Nominal magnet operation is about 30 amperes. Magnet data was taken at 20, 30, and 40 amperes to understand the effects of saturation on the field index, n .

We normalized the measured field profile for the three different operating currents: 20, 30, and 40 Amperes. Each field profile, as one would expect, had a peak field at $r = 0$. The data was linearly scaled to bring this peak field to unity. The simultaneous plotting of these normalized profiles, as shown in Figure 2, confirms that the field index's (n 's) profile does not vary with field strength, even into the beginning of the saturated régime. This generously allows for just one analysis of the field profile.

The LANL Finite Element code Possion Superfish's (PSF) [6] output was compared to our measurement. Strong agreement between the McClain & Friedman's measurement with the PSF justified the use of the computer model for further analysis, see figure 3. [3]

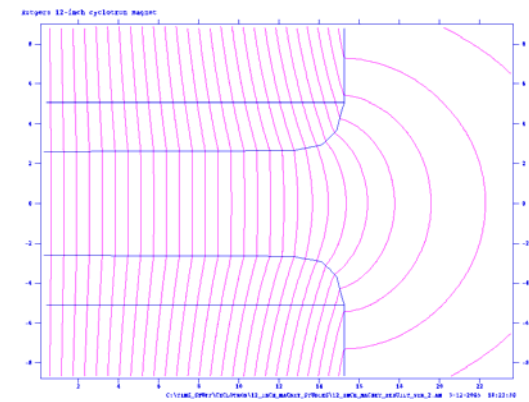


Fig.3 PSF model of 12-inch magnet tapered tips.

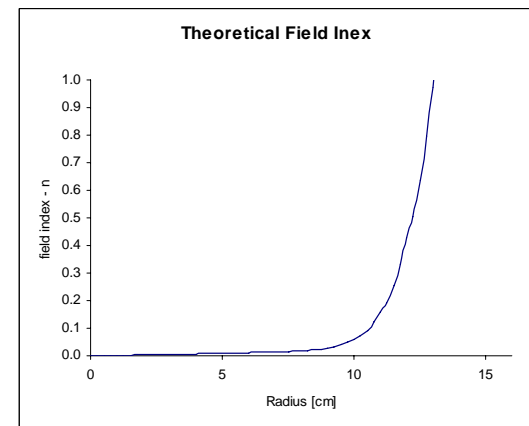


Fig.4 PSF Modeled field index, n , as a function of radius.

The field index, n , as a function of radius was determined by the PSF model and plotted in figure 4. As show above in section II, n will be needed for calculating the expected betatron frequency.

IV. ION SOURCE & FARADAY CUP.

Significant improvement to the operation of the cyclotron has come from the installation of a chimney to the ion source and replacement of the Faraday cup.

The ion source chimney allows thermionic electrons to freely leave the biased filament following the vertical magnetic field lines to the median plane all the while ionizing hydrogen. Admission of hydrogen gas to the enclosed volume of the filament and chimney improved vacuum performance. A 1/16-inch aperture in the chimney wall located at the height of the median plane launches the protons directly into the DEE as pictured in figure 6.

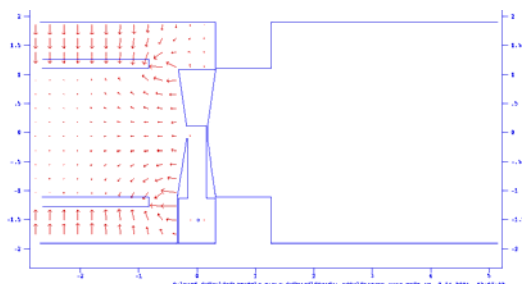


Fig. 5 PSF model of E-fields at the ion source.

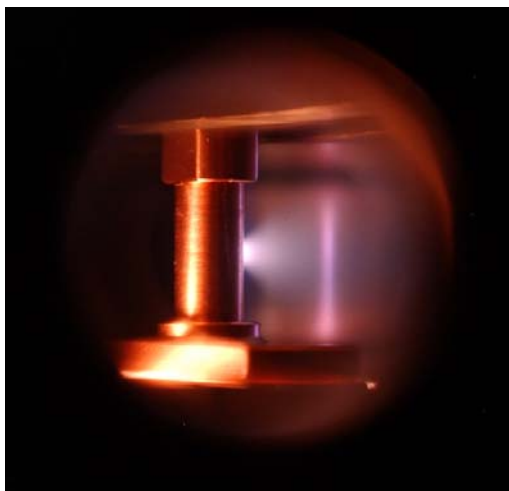


Fig. 6 Ion Source with chimney in operation

It was calculated that the required RF power for the first revolutions of ions to clear the chimney (with the cyclotron operation at 14.900MHz) was 165 watts as plotted in figure 7. [4,7]

Confirmation of the ions source model came from establishing beam with 300 watts of RF power and slowly decreasing RF power. Beam intensity decreased with decreasing RF power, but at 170 watts the beam current abruptly dropped to zero.

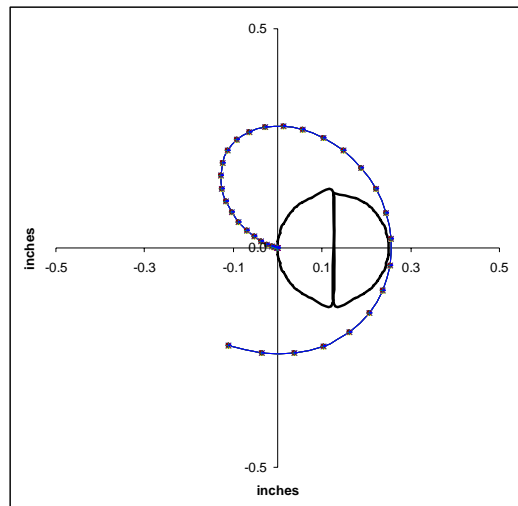


Fig 7 Calculation showing first ions squireak by at 165 Watts of RF into the cyclotron at 14.900MHz.

The faraday cup, shown in figure 8, used up to this point utilized a cap to shield the electrometer from the leaked RF fields. This caps thickness was greater than the turn-to-turn spacing of the ion revolutions at a radius greater than 2.1 inches when operating at 14.900MHz with a DEE voltage of 7,500 V_{p-p} . Such a thick tip would prevent the ions from hitting the sensitive portion of the ion collector, rather the ions would just return to chassis ground. A new, simpler, Faraday cup was installed. It simply consists of an unshielded aluminum block. RF suppression was still a concern, so externally a notch filter, with -100dB of rejection at 14.900MHz, was installed in the Faraday cup line that connects to the electrometer. An RF choke was also installed in this line, just before the electrometer connection.



Fig. 8 Displaying older Faraday collector showing thick RF shielded tip (left) and the fluorescent screen at the bottom right). Ion rotation is obviously CCW (counter clockwise).

V. BETATRON MOTION OBSERVED.

Finally, with the orchestra of the tapered pole tips, chimney based ion source, and improved Faraday cup, we set forth to produce beam. Initial beam indication came from monitoring the beam current on the electrometer. The fluorescent screen was retracted.

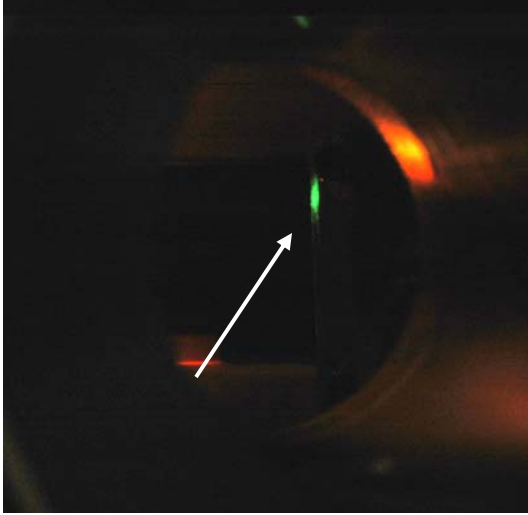


Fig 9 Beam spot on florescent screen.

The operational sequence was as follows: pump the cyclotron chamber below 1E-5 Torr, shut off ion gauge, turn on the magnet with approximately 20 amps of excitation current, turn on filament bias supply (-200V), then slowly ramp filament heater supply until thermionic emission on order of 10mA is reached, slowly admit hydrogen gas until an increase in emission current was noted. Final optimal filament heater current is noted at 20.6 Amps (for 0.015 inch diameter 1% Th-W wire) and final optimal leak dial setting of 104 was recored. RF was turned on at a low level and tuned to resonance (found to be 14.8640 MHz), the RF drive was increase to 300 watts – corresponding to 7,500 V_{p-p} on the DEE. To satisfy the “cyclotron resonance condition” the magnet current was slowly swept up while monitoring the electrometer needle for deflection. Almost immediately a strong signal was detected. Precise “tuning” of the magnetic field yielded a peak beam current reading of 20nAmps. After the electrometer reading stabilized, the faraday cup was retracted and the florescent screen inserted. Instantly a visible beam spot appeared. Adjustment of the magnetic field, the RF power level or the RF frequency modulated the intensity, position and shape of the of the beam spot.

The beam spot initially observed, figure 9, was clearly above the median plane, and so the florescent screen – mounted on a linear positioner - was radially adjusted. Again the beam spot wandered. We then set the camera to a 15 second exposure and scanned the florescent screen slowly. The resulting image, Fig 10, clearly showed periodic behavior about the median plane with increasing frequency and decreasing amplitude as r increased. This was immediately identified as betatron motion.

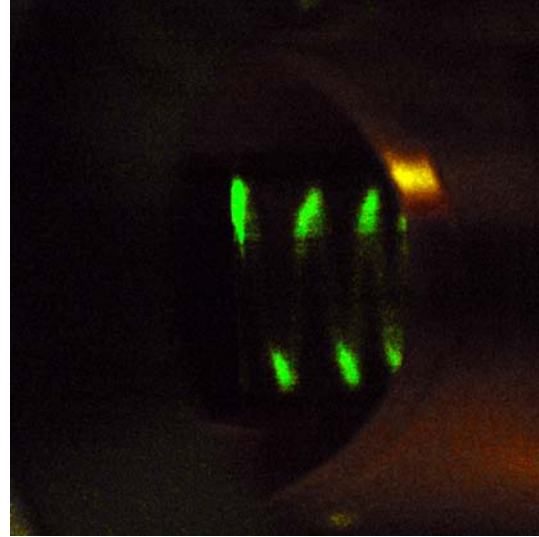


Fig. 10 Observed Vertical Betatron Oscillations. Ion source is to the left and radius increases to the right.

The radial position of several peaks from the observed vertical betatron motion were recorded:

| | |
|------------------------|----------|
| $r_0 = 8.6 \text{ cm}$ | (338keV) |
| $r_1 = 9.2 \text{ cm}$ | (387keV) |
| $r_2 = 9.6 \text{ cm}$ | (421keV) |

Relevant operating conditions:

| | |
|-----------------------------|-------------------------------|
| $f_0 = 14.8640 \text{ MHz}$ | ($B = 0.977 \text{ Tesla}$) |
| RF power = 300 Watts | |
| Magnet Current = 28.28 Amps | |

VI. EXPECTED BETATRON MOTION.

Returning to the energy equation of cyclotron motion we can first determine the turn-to-turn spacing of the ions as a function of radius:

$$E = \frac{qB^2}{2m} r^2 \text{ or}$$

$$E = \alpha^2 r^2 \text{ where } \alpha^2 = \frac{qB^2}{2m}$$

Solve for $r(E)$ to get:

$$r(E) = \frac{1}{\alpha} \sqrt{E}$$

Differentiate with respect to E:

$$\frac{\partial r(E)}{\partial E} = \frac{1}{\alpha} \frac{\partial}{\partial E} \sqrt{E} = \frac{1}{2\alpha\sqrt{E}}$$

So,

$$\Delta r(E) = \frac{\Delta E}{2\alpha\sqrt{E}}$$

Where ΔE is the energy (in eV) gained in one revolution (just the DEE V_{p-p}). Also E is a function of r , so we can transform $\Delta r(E) \rightarrow \Delta r(r)$:

$$\Delta r(E) = \frac{\Delta E}{2\alpha\sqrt{E}} \Rightarrow$$

$$\Delta r(r) = \frac{\Delta E}{2\alpha\sqrt{\alpha^2 r^2}} = \frac{\Delta E}{2\alpha^2 r}$$

Replacing α we get:

$$\Delta r(r) = \frac{\Delta E m}{qB^2 r}$$

Operating at 300 Watts of RF power on resonance at 14.8640 MHz (Corresponding to a B-field of 0.977 Tesla), the DEE V_{p-p} that develops is 7,500 V, thus ΔE is 7,500eV. Taking $q=1.6E-19$, and $m=1.67E-27$, so we can expect:

$$\Delta r(r) = \frac{(7500eV)(1.67E-27)}{(1.6E-19)(0.977)^2} \frac{1}{r} \text{ or}$$

$$\Delta r(r) = (8.2E-5) \frac{1}{r}$$

We recall from section II that the vertical betatron frequency follows the square root of the field index multiplied by the RF frequency:

$$f_{\beta\text{-vert}} = \sqrt{n} f_0$$

We extend that relationship to their respective periods of oscillation:

$$T_{\beta\text{-vert}} = \frac{1}{\sqrt{n}} T_0$$

Thus for a given n it take $\frac{1}{\sqrt{n}}$ RF periods or ion

revolutions to complete one vertical betatron oscillation.

What remains is to determine n at a given peak, and follow the n 's evolution in a piecewise fashion to the next betatron peak. Lets start by taking the first noted peak r_0 (of section V) of 8.6 cm, from the PSF study we determine n in the region between 8 and 10 cm:

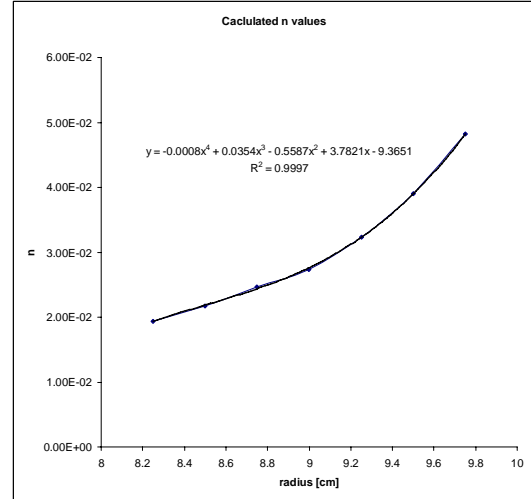


Fig.11 field index, n , between 8 & 10 cm.

Using a fourth order polynomial fit and our equation for $\Delta r(r)$ we can create table 1. The first measured peak of the vertical betatron oscillation was at $r_0 = 8.6$ cm, and we denote that as the start of the betatron period. We then allow one RF period, hence one ion revolution, to process, after which, using our equation for $\Delta r(r)$, we reevaluate the new radius and that radius' field index n . It can easily be shown that the fraction that the betatron period advances at a given n is just \sqrt{n} .

| r [cm] | n(r) | Fraction of Betatron Period |
|---------------------|-----------------------|-----------------------------|
| 8.6 | 0.025 | 0 |
| 8.7 | 0.026 | 0.2 |
| 8.8 | 0.026 | 0.3 |
| 8.9 | 0.027 | 0.5 |
| 9.0 | 0.028 | 0.6 |
| 9.1 | 0.030 | 0.8 |
| 9.2 | 0.031 | 1.0 |
| 9.2 | 0.033 | 1.2 |
| 9.3 | 0.034 | 1.3 |
| 9.4 | 0.037 | 1.5 |
| 9.5 | 0.039 | 1.7 |
| 9.6 | 0.041 | 1.9 |
| 9.7 | 0.042 | 2.1 |

Table 1. Theoretical betatron advance per ion revolution.

Integer values of fractional betatron periods indicate the full completion of a vertical betatron oscillation. These "integer" values are

underlined and highlighted in blue in table 1. Noting the radii at which these occur the reader immediately sees the same values that were observed at r_1 and r_2 as reported in section V. It should be pointed out that the vertical betatron period “spacing” decreasing with increasing radius as is seen in figure 10.

VII. BETATRON INITIAL CONDITIONS.

The natural question that should be asked: if the ion source aperture is in the median plane, why then the large vertical displacement? This can be attributed to the early ions sensitivity to any vertical component of the electrical field. Inspection of Fig 5 shows that the electric field from the ion source into the DEE diverges quickly. Thus a slight offset of the DEE with respect to the median plane will provide a significant vertical component. This can be mitigated by the installation of “pullers” on the DEE’s aperture in the region of the ion source – a possible student project.

VIII. CONCLUSIONS. Successful operation of the cyclotron with the 12-inch magnet was finally demonstrated. Unexpectedly, betatron motion was clearly observed, and the analysis of which confirms the designed operation of the weak focusing pole tips. Radial betatron oscillations were not noticed as their period in the regime of low field index n is comparable to that of the ion revolution frequency.

IX. ACKNOWLEDGEMENTS. The authors would like to thank Prof. Mohan Kalelkar for finding the required financial support to make this work possible. Additionally, we thank Prof’s Gershenson, Thomson, and Kojima for lending the talent of their best students each year for over five years.

X. REFERENCES:

[1] Toni Feder “Building a Cyclotron on a Shoe string.” *Physics Today*, November 2004, pages 30 - 31

[2]http://www.physics.rutgers.edu/cyclotron/papers/Profiling_the_Magnetic_Field_of_the_New_Pole_Tips.pdf

[3]http://www.physics.rutgers.edu/cyclotron/papers/12_inch_magnet_studies_4.pdf

[4]http://www.physics.rutgers.edu/cyclotron/papers/ion_source_studies_part_1.pdf

[5]J.J. Livingood, “Principles of Cyclic Particle Accelerators” D. Van Nostrand, 1961

[6]http://laacg.lanl.gov/laacg/services/serv_access.shtml

[7]http://www.physics.rutgers.edu/cyclotron/papers/12_inch_dee_voltage.pdf